Bioorganic & Medicinal Chemistry 21 (2013) 1621–1627

Contents lists available at SciVerse ScienceDirect

Bioorganic & Medicinal Chemistry

journal homepage: www.elsevier.com/locate/bmc

Novel leucine ureido derivatives as inhibitors of aminopeptidase N (APN)

Chunhua Ma, Kang Jin, Jiangying Cao, Lei Zhang, Xiaoguang Li, Wenfang Xu *

Department of Medicinal Chemistry, School of Pharmaceutical Sciences, Shandong University 44, West Culture Road, Jinan 250012, PR China

ARTICLE INFO

Article history:
Received 31 December 2012
Revised 30 January 2013
Accepted 31 January 2013
Available online 9 February 2013

Keywords:
Aminopeptidase N
Inhibitors
Leucine ureido derivatives
Synthesis

ABSTRACT

Aminopeptidase N (APN/CD13) over expressed on tumor cells, plays a critical role in tumor invasion, metastasis, and tumor angiogenesis. Here we described the design, synthesis and preliminary activity studies of novel leucine ureido derivatives as aminopeptidase N (APN/CD13) inhibitors. The results showed that compound **8c** had the most potent inhibitory activity against APN with the IC_{50} value to 0.06 ± 0.041 μM, which could be used for further anticancer agent research.

1. Introduction

Aminopeptidase N (APN; EC 3.4.11.2) is a zinc-dependent type II membrane-bond ectopeptidase,[1] which preferentially releases neutral and basic amino acids from the N-terminus of oligopeptides.[2] Scientific research has been found that APN is over-expressed on tumor cells and plays key roles in extracellular matrix degradation, tumor cell invasion and tumor angiogenesis.[3,4] Therefore, APN was regarded as an attractive target for anti-cancer drug design.

Since 1976, several natural and small molecule inhibitors of APN have been found, for example, Bestatin,[5] Probestin,[6] Amastatin,[7] Actinonin,[8] Phebestin,[9] Lapstatin,[10] AHPA-Val,[11] Leuhistin,[12] and so on. Among them, Bestatin has been launched and is widely employed clinically as an anti-tumor agent. Our group has previously reported several kinds of synthetic APN inhibitors, such as L-lysine derivates,[13] 1,3,4-thiadiazole derivates,[14] L-iso-glutamine derivatives,[15] chloramphenicol amine derivatives,[16] L-arginine derivatives,[17] indoline-2,3-dione derivates[18] and ureido derivatives.[19]

In our previous work, a series of ureido derivatives was reported as potent APN inhibitors. Some of them showed potential inhibitory activities against APN. Especially, compound **4k**, whose IC_{50} was 2.7 μM compared with 9.1 μM of Bestatin.[20] Herein, in order to find better APN inhibitors, we used compound **4k** as the leading compound. In our series of L-arginine derivatives, we found that the compounds contained *ortho*-substituted phenyl groups have better activities than those contained unsubstituted.[17] And we also found that a substituent in *meta*-position such as chlorine, fluorine, bromine, or methane could enhance the potency of inhibitors in our series of indoline-2,3-dione derivatives.[18] Based on these reasons, a series of novel leucine ureido derivatives which containing different *meta*- or *ortho*-substituents on the phenyl group of **4k** have been synthesized, while, some analogues with substituted benzyl groups also have been obtained (Fig. 1). The activity results and analysis of structure–activity relationship (SAR) were also shown in this article.

2. Chemistry

The target compounds **8a–8g** and **10a–10d** were synthesized efficiently via the route outlined in Scheme 1. Starting from commercially available L-leucine, the key intermediate leucine isocyanate was obtained via esterification and isocyanate, and then coupled with the corresponding *ortho*-substituted anilines or benzylamines. Without further purification, they were directly transformed into hydroxamic acids as the target products. The main synthetic methods of target compounds **9a–9g** and **11a–11b** are shown in Scheme 2. With corresponding *meta*-substituted anilines or benzylamines, as the raw materials, they were converted into isocyanates, and then coupled with leucine methyl esters, to obtain the ureido linker. Finally the methyl ester was transformed into hydroxamic acids as the target compounds.

* Corresponding author. Tel./fax: +86 531 88382264.
E-mail address: wfxu@yahoo.cn (W. Xu).

0968-0896/$ - see front matter © 2013 Elsevier Ltd. All rights reserved.
http://dx.doi.org/10.1016/j.bmc.2013.01.068

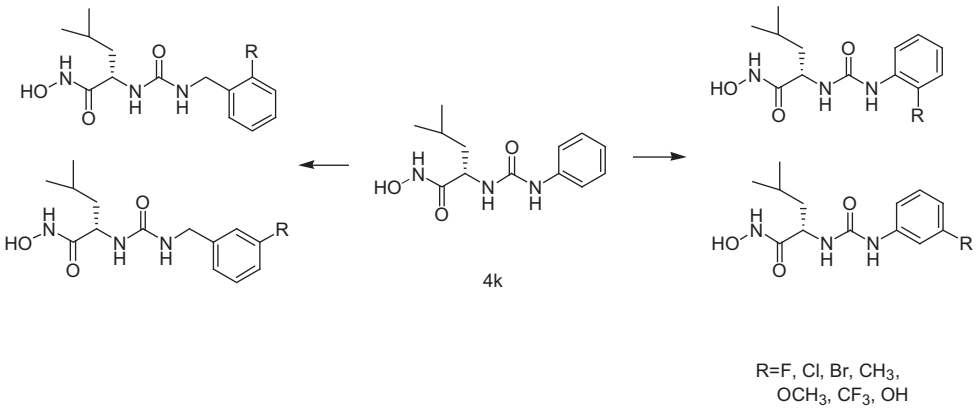

Figure 1. The new APNIs derived from compound **4k**.

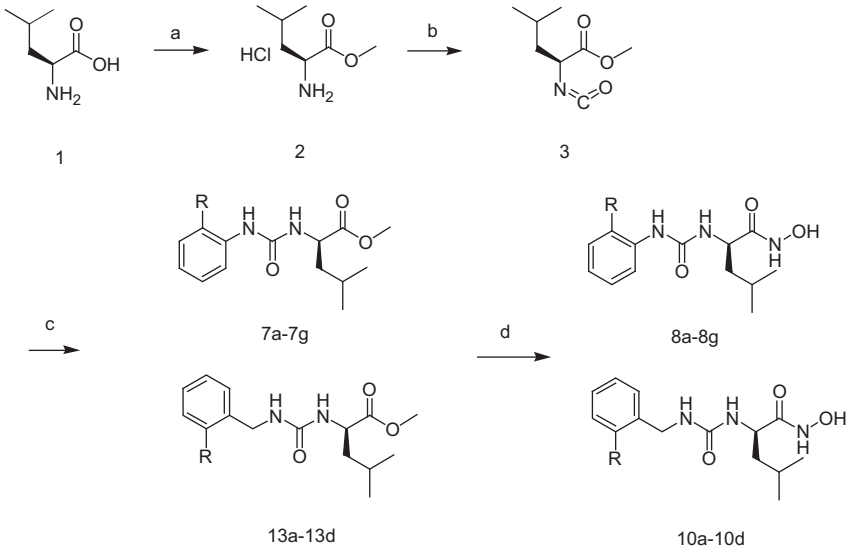

Scheme 1. Reagents and conditions: (a) acetyl chloride, MeOH, reflux; (b) triphosgene, $NaHCO_3$, DCM, ice-bath; (c) corresponding *ortho*-substituted anilines or benzylamines, DCM, room temperature; (d) NH_2OK, MeOH, 1 h.

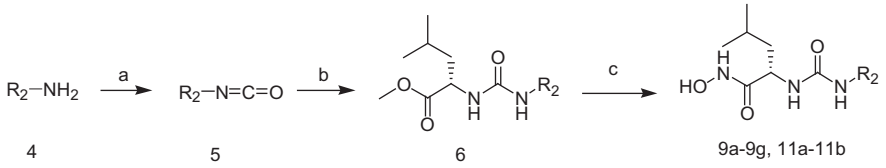

Scheme 2. Reagents and conditions: (a) triphosgene, toluene, reflux; (b) methyl ester hydrochlorides of L-Leu and DCM, Et_3N, room temp, 1–2 h; (c) NH_2OK, MeOH, 1 h.

3. Results and discussion

The target compounds were evaluated for their inhibitory activities toward APN/CD13 and HDACs. Similar to APN, HDACs are zinc-dependent metalloproteinase as well and associated closely with the invasion and metastasis of tumor. Thereby the assay was performed on both of APN and HDACs so as to identify their selectivity, all the inhibition results are summarized in Tables 1–3. Bestatin was used as the positive control to APN, while, SAHA was used for HDACs.

As shown in Tables 1–3, it is worthy to note that these ureido derivatives displayed a better enzymatic inhibition towards APN compared with HDACs, with IC_{50} values lying in micromole level. These results, to a certain extent, validated our strategy for rational designing of potential APNIs. As the above mentioned selectivity against APN, the following SARs were mainly discussed about APN inhibition.

Among these inhibitors, generally speaking, compounds with *ortho*-substituents of phenyl group showed better activity than the leading compound **4k**. The possible reason may be due to the substituent groups enhancing the interaction with the hydrophobic region of the enzyme. Comparing **8a–8d** and **10a–10d**, we can find the activity of substituted anilines is better than benzylamines, it is reason may be the length between benzene ring of aniline to hydroxamic acid is more similar to the length between hydrophobic region and zinc ion. Comparing **8a–8g** and **9a–9g**, we could find that the compounds contained *ortho*-substituted phenyl groups have better activities than those contained

Table 1
The structures and inhibitory activities of the target compounds **8a–8g** against APN and HDACs

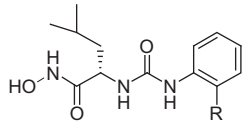

Compd	R	IC_{50}[a] (μM) APN	IC_{50}[a] (μM) HDACs
8a	F	0.52 ± 0.064	>100
8b	Cl	0.093 ± 0.120	>100
8c	Br	0.06 ± 0.041	>100
8d	CH_3	0.18 ± 0.032	>100
8e	OCH_3	0.13 ± 0.027	>100
8f	CF_3	0.79 ± 0.163	>100
8g	OH	11.9 ± 1.078	>100
Beststin	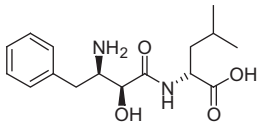	3.40 ± 0.028	>100
4k	H	1.15 ± 0.528	>100
SAHA	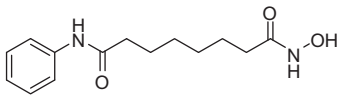	—	0.12 ± 0.03

[a] Mean values and standard deviations of triplicate experiments are given.

Table 2
The structures and inhibitory activities of the target compounds **9a–9g** against APN and HDACs

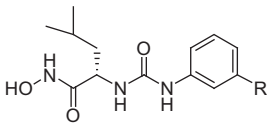

Compd	R	IC_{50}[a] (μM) APN	IC_{50}[a] (μM) HDACs
9a	F	1.90 ± 0.258	>100
9b	Cl	1.66 ± 0.153	>100
9c	Br	0.58 ± 0.060	>100
9d	CH_3	0.24 ± 0.234	>100
9e	OCH_3	1.36 ± 0.342	>100
9f	CF_3	1.97 ± 0.324	>100
9g	OH	1.70 ± 1.890	>100
Beststin	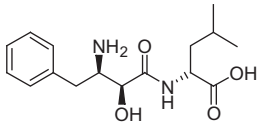	3.40 ± 0.028	>100
4k	H	1.15 ± 0.528	>100
SAHA	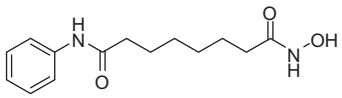		0.12 ± 0.03

[a] Mean values and standard deviations of triplicate experiments are given.

meta-substituted phenyl groups. Comparing compounds **8a–8g** with *ortho*-substituted at phenyl groups, the APN inhibitory activities were different with the substitutions on the aromatic ring. The data shown in Table 1 suggested that the preferred substitutions against APN were, in decreasing order, halogen-substitution, methoxy-substitution, methane-substitution and hydroxy-substitution. And different halogens in aromatic ring also have different levels of impacts on their activities. The compounds with a bromide group on the benzene ring (**8c**) were more potent than others containing a chloride substituent (**8b**), followed by the fluorinate inhibitors (**8a**) at last. The possible reason may be due to the bigger volume hydrophobic substitution can enhance the interaction with the hydrophobic region of the enzyme. In another way, compound **8f** with trifluoromethyl-group showed worse activity than compound **8c**, it seems that too big bulk leads to impaired activity, suggesting there is a space requirement in the binding pockets to accommodate the suitable substituents. Compound with hydroxy-substitution (**8g**) on the aromatic ring show the least APN inhibitory activities, which may reveal hydrophilic groups diminish activities of compounds.

Table 3
The structures and inhibitory activities of the target compounds **10a**–**10d** and **11a**–**11b** against APN and HDACs

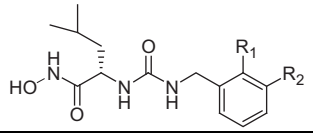

Compd	R1	R2	IC_{50}[a] (μM) APN	IC_{50}[a] (μM) HDACs
10a	F	H	1.38 ± 0.246	>100
10b	Cl	H	0.22 ± 0.124	>100
10c	Br	H	0.13 ± 0.036	>100
10d	CH_3	H	0.90 ± 0.235	>100
11a	H	Cl	0.35 ± 0.215	>100
11b	H	CH_3	0.44 ± 0.165	>100
Beststin	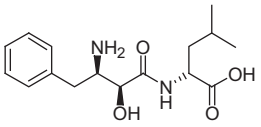		3.40 ± 0.028	>100
4k	H		1.15 ± 0.528	>100
SAHA	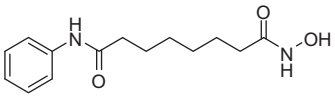			0.12 ± 0.03

[a] Mean values and standard deviations of triplicate experiments are given.

The most active compounds are **8c**, which had a better inhibition (IC_{50} = 0.06 ± 0.041 μM) than leading compound and control Bestatin (IC_{50} = 3.40 ± 0.028 μM). Compounds **8b**, **8d**, **8e**, **10b** and **10c** also have considerable activities (IC_{50} = 0.093, 0.18, 0.13, 0.22 and 0.13 μM, respectively).

Furthermore, we assessed the ability of some compounds with the nanomolar range for enzymatic inhibition on the human APN deriving from cultured **ES-2** human ovarian clear cell carcinoma cells high-expressing APN. Results were presented in Figure 2, from which we can see that all these compounds were still better than Bestatin (20.12 ± 1.265 μM), some even with more than 10-fold improvement, and **8c** showed the best capability (IC_{50} = 0.53 ± 0.116 μM). Similar to the above enzyme inhibitory activity, the human APN inhibition of these compounds also presented consistent trends.

Additionally, compounds **8b**, **8c**, **8e** are detected for their potential effects on proliferation of two tumor cell lines (**ES-2** and **U-937** cells) with Bestatin as control via MTT assay. The result depicted in Table 4 indicated that all compounds' anti-proliferative effects against **ES-2** cells are better than against **U-937** cells mainly owing to APN's higher expression level on **ES-2** cells than the other. Compound **8c** shows the best effect against **ES-2** cells with the IC_{50} of 405 ± 0.08 μM complying with the enzymatic assay.

Aiming to investigate the interaction between the target compounds and APN, the most active compound **8c**, was chosen to be constructed using a Sybyl/Sketch module and optimized via Powell's method by the Tripos force field with convergence criterion set at 0.05 kcal/(Å mol), and assigned with the Gasteiger–Hückel method. The docking study of **8c** and the active site of APN was performed using Sybyl/FlexX module. The active site was defined as 10.0 Å radius circles around Bestatin in the co-crystal structure (PDB code: 4YFR). Other docking parameters utilized in the program were remained default. The result showed in Figure 3 a suggested that phenyl group can insert into S1 pocket and the hydroxamic acid group can chelate with the zinc ion which was the crucial catalytic factor in active site. In addition, a 2D pattern of detailed binding mode was created as well (Fig. 3b). The phenyl group of compound **8c** can form hydrophobic interaction with Phe472 of S1 pocket, while, the ureido group and hydroxamic acid group can from hydrogen bonds with Gln213, Ala353 and Gln213, Glu355, Glu411, Tyr477, respectively.

Although the computed information partially supported our assumption, the exact binding model of 8c with APN should be ob-

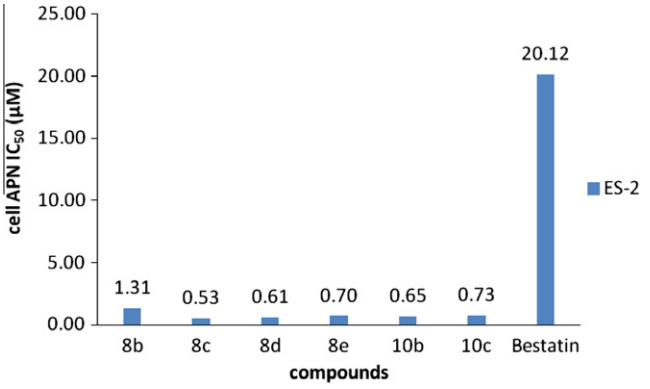

Figure 2. Inhibitory activity of compounds **8b**, **8c**, **8d**, **8e**, **10b**, **10c** and Bestatin against APN on **ES-2** cells. Data expressed are mean values of three independent experiments.

Table 4
The structures and cell proliferation IC_{50} values of some target compounds toward **ES-2** and **U-937**

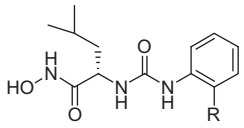

Compd	R	IC_{50}[a] (μm) towards **ES-2**	IC_{50}[a] (μm) towards **U-937**
8b	Cl	615	>1000
8c	Br	405	>1000
8e	OCH_3	480	>1000
Bestatin	—	620	>1000

[a] Mean values and standard deviations of triplicate experiments are given.

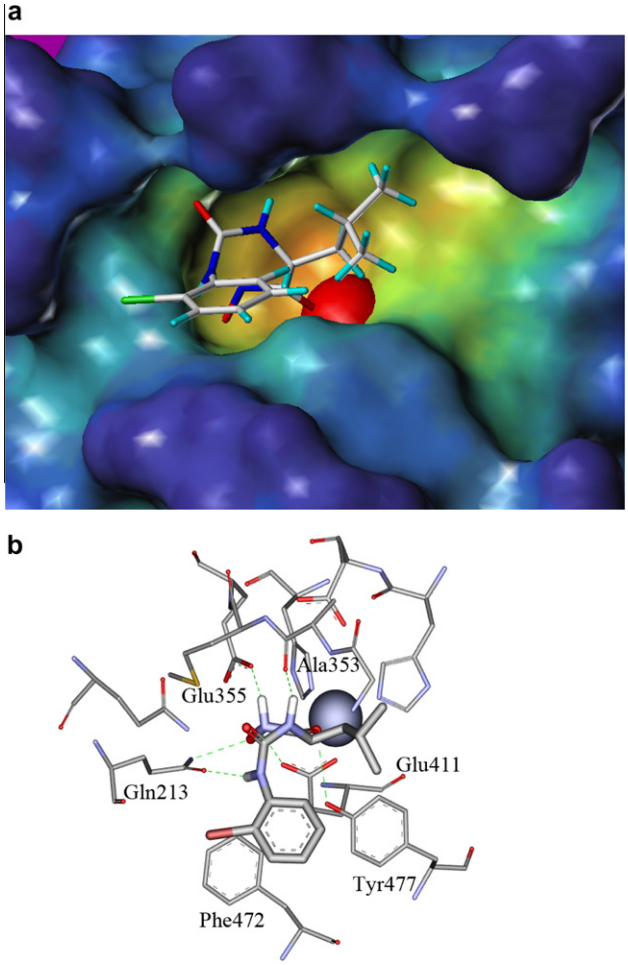

Figure 3. (a) The FlexX docking result of **8c** with APN (PDB: 4YFR). (b) The docking result of **8c** shown by LIGPLOT

tained from further X-ray crystal studies, which is under research in our lab.

4. Conclusions

In all, one series of novel potent leucine ureido derivative as APN inhibitors have been synthesized and evaluated. The preliminary results showed that most of the target compounds exhibited better inhibition than the control Bestatin and the leading compound **4k**. These results suggest that leucine ureido derivatives could possess good inhibitory activities after substitution introduced in *ortho*-position of phenyl group, which could be used as new lead for further structure transformation in the future APNIs exploration.

5. Experiment

5.1. Chemistry: general procedures

All the materials involved were purchased from commercial suppliers. Solvents were distilled prior to use. All the reactions were monitored by thin-layer chromatography on 0.25 mm silica gel plates (60GF-254) and visualized with UV light, or chloride ferric. The products were purified by column chromatography which was performed using 200–300 mesh silica gel. NMR spectra were determined on a Brucker Avance 600 spectrometer, δ in parts per million and J in Hertz. TMS was used as an internal standard. ESI-MS were determined on an API 4000 spectrometer. Measurements were made in DMSO-d_6 solutions. Melting points were tested using an electrothermal melting point apparatus and were uncorrected.

5.2. General procedure for the synthesis of 8a–8g and 10a–10d

To a mixture of L-leucine methyl ester hydrochloride (3.62 g, 20 mmol) in saturated $NaHCO_3$ (72 mL) and DCM (72 mL) was added triphosgene (1.96 g, 6.6 mmol). The reaction mixture was vigorously stirred under ice-water bath for 1 h and the organic layer was collected. The water layer was extracted with DCM for three times and the organic phase was combined and dried with $MgSO_4$. After the solvent removed under vacuum, the residue was dissolved in DCM (20 mL). This solution was then added to corresponding *ortho*-substituted anilines or benzylamines (21 mmol) in DCM (80 mL) under ice bath. The reaction mixture was stirred at room temperature for 12 h and then the solvent was removed under low pressure. The residue was taken up with ethyl acetate (100 mL) and washed with 1 N HCl (30 mL) and brine (30 mL). The organic phase was dried with $MgSO_4$. After the solvent removed, the residue without purification was directly added to a solution of potassium hydroxylamine (8.37 g, 56 mmol) in methanol (20 mL). The reaction mixture was stirred at room temperature for 1 h and then removed methanol under low pressure. The residue was taken up with 1 N HCl and extracted with ethyl acetate. The organic phase was washed with brine and dried with $MgSO_4$. After the solvent removed under low pressure, the residue was separated by silica gel column chromatography to afford **8a**–**8g** and **10a**–**10d**, respectively.

5.2.1. (*S*)-2-[3-(2-Fluoro-phenyl)-ureido]-4-methyl-pentanoic acid hydroxyamide (8a)

White powder, yield 43%, mp = 172–174 °C; ^{1}H NMR (600 MHz, DMSO-d_6) δ 10.70 (s, 1H), 8.76 (s, 1H), 8.35 (s, 1H), 8.10 (t, 1H, J = 6.0 Hz), 7.15 (m, 1H), 7.06 (d, 1H, J = 6.0 Hz), 6.92 (m, 1H), 4.13 (m, 1H), 1.59 (m, 1H), 1.42 (t, 2H, J = 7.2 Hz), 0.89 (dd, 6H, J = 6.6, 10.8 Hz); HRMS (AP-ESI) m/z Calcd for $C_{13}H_{18}FN_3O_3$ $[M+H]^+$ 284.1405. Found, 284.1404.

5.2.2. (*S*)-2-[3-(2-Chloro-phenyl)-ureido]-4-methyl-pentanoic acid hydroxyamide (8b)

White powder, yield 51%, mp = 163–164 °C; ^{1}H NMR (600 MHz, DMSO-d_6): δ 10.80 (s, 1H), 8.87 (s, 1H), 8.15 (m, 2H), 7.39 (dd, 1H, J = 1.2, 7.2 Hz), 7.36 (d, 1H, J = 9.0 Hz), 7.23 (t, 1H, J = 7.2 Hz), 6.94 (t, 1H, J = 7.2 Hz), 4.18 (m, 1H), 1.58 (m, 1H), 1.42 (t, 2H, J = 7.2 Hz), 0.89 (dd, 6H, J = 6.6, 10.8 Hz); HRMS (AP-ESI) m/z Calcd for $C_{13}H_{18}ClN_3O_3$ $[M+H]^+$ 300.1109. Found, 300.1110.

5.2.3. (*S*)-2-[3-(2-Bromo-phenyl)-ureido]-4-methyl-pentanoic acid hydroxyamide (8c)

White powder, yield 49%, mp = 182–184 °C; ^{1}H NMR (600 MHz, DMSO-d_6): δ 10.81 (s, 1H), 8.88 (s, 1H), 8.06 (d, 1H, J = 7.8 Hz), 7.98 (s, 1H), 7.55 (d, 1H, J = 7.8 Hz), 7.43 (d, 1H, J = 9.0 Hz), 7.27 (t, 1H, J = 7.8 Hz), 6.89 (t, 1H, J = 7.8 Hz), 4.15 (m, 1H), 1.59 (m, 1H), 1.42 (t, 2H, J = 7.2 Hz), 0.89 (dd, 6H, J = 6.6, 10.8 Hz); HRMS (AP-ESI) m/z Calcd for $C_{13}H_{18}BrN_3O_3$ $[M+H]^+$ 344.0604. Found, 344.0598.

5.2.4. (*S*)-4-Methyl-2-(3-*o*-tolyl-ureido)-pentanoic acid hydroxyamide (8d)

White powder, yield 47%, mp = 184–186 °C; ^{1}H NMR (600 MHz, DMSO-d_6): δ 10.80 (s, 1H), 8.88 (s, 1H), 7.85 (d, 1H, J = 8.4 Hz), 7.11 (d, 1H, J = 7.2 Hz), 7.07 (t, 1H, J = 7.8 Hz), 6.86 (m, 2H), 4.18 (m, 1H), 2.17 (s, 3H), 1.58 (m, 1H), 1.41 (t, 2H, J = 7.2 Hz), 0.89 (dd, 6H,

J = 6.6, 8.4 Hz); HRMS (AP-ESI) m/z Calcd for $C_{14}H_{21}N_3O_3$, $[M+H]^+$ 280.1656. Found, 280.1654.

5.2.5. (*S*)-2-[3-(2-Methoxy-phenyl)-ureido]-4-methyl-pentanoic acid hydroxyamide (8e)

White powder, yield 43%, mp = 170–172 °C; ^{1}H NMR (600 MHz, DMSO-d_6): δ 10.79 (s, 1H), 8.82 (s, 1H), 8.09 (s, 1H), 8.06 (dd, 1H, J = 1.2, 7.2 Hz), 7.15 (d, 1H, J = 9.0 Hz), 6.95 (d, 1H, J = 7.2 Hz), 6.86 (t, 1H, J = 7.2 Hz), 6.82 (t, 1H, J = 7.2 Hz), 4.12 (m, 1H), 3.82 (s, 3H), 1.58 (m, 1H), 1.40 (t, 2H, J = 7.2 Hz), 0.89 (dd, 6H, J = 6.6, 10.8 Hz); HRMS (AP-ESI) m/z Calcd for $C_{14}H_{21}N_3O_4$, $[M+H]^+$ 296.1605. Found, 296.1604.

5.2.6. (*S*)-4-Methyl-2-[3-(2-trifluoromethyl-phenyl)-ureido]-pentanoic acid hydroxyamide (8f)

White powder, yield 45%, mp = 179–180 °C; ^{1}H NMR (600 MHz, DMSO-d_6): δ 10.81 (s, 1H), 8.85 (s, 1H), 7.94 (m, 2H), 7.61 (d, 1H, J = 7.8 Hz), 7.56 (t, 1H, J = 7.8 Hz), 7.37 (d, 1H, J = 7.8 Hz), 7.18 (t, 1H, J = 7.2 Hz), 4.18 (m, 1H), 1.58 (m, 1H), 1.42 (t, 2H, J = 7.2 Hz), 0.89 (dd, 6H, J = 6.6, 10.8 Hz); HRMS (AP-ESI) m/z Calcd for $C_{14}H_{18}F_3N_3O_3$, $[M+H]^+$ 334.1373. Found, 334.1373.

5.2.7. (*S*)-2-[3-(2-Hydroxy-phenyl)-ureido]-4-methyl-pentanoic acid hydroxyamide (8g)

White powder, yield 48%, mp = 146–148 °C; ^{1}H NMR (600 MHz, DMSO-d_6): δ 10.65 (s, 1H), 9.70 (s, 1H), 8.73 (s, 1H), 8.02 (s, 1H), 7.84 (d, 1H, J = 7.8 Hz), 7.04 (d, 1H, J = 7.8 Hz), 6.72 (m, 3H), 4.12 (m, 1H), 1.61 (m, 1H), 1.42 (t, 2H, J = 7.2 Hz), 0.89 (dd, 6H, J = 6.6, 10.8 Hz); HRMS (AP-ESI) m/z Calcd for $C_{14}H_{19}N_3O_4$, $[M+H]^+$ 282.1448. Found, 282.1449.

5.2.8. (*S*)-2-[3-(2-Fluoro-benzyl)-ureido]-4-methyl-pentanoic acid hydroxyamide (10a)

White powder, yield 51%, mp = 164–166 °C; ^{1}H NMR (600 MHz, DMSO-d_6): δ 10.68 (s, 1H), 8.80 (s, 1H), 7.58 (d, 1H, J = 7.8 Hz), 7.36 (m, 1H), 7.29 (d, 1H, J = 6.0 Hz), 7.19 (t, 1H, J = 7.2 Hz), 6.48 (t, 1H, J = 6.0 Hz), 6.30 (d, 1H, J = 9.0 Hz), 4.22 (d, 2H, J = 6.0 Hz), 4.08 (m, 1H), 1.54 (m, 1H), 1.36 (t, 2H, J = 7.2 Hz), 0.86 (dd, 6H, J = 6.6, 10.8 Hz); HRMS (AP-ESI) m/z Calcd for $C_{14}H_{20}FN_3O_3$, $[M+H]^+$ 298.1561. Found, 298.1563.

5.2.9. (*S*)-2-[3-(2-Chloro-benzyl)-ureido]-4-methyl-pentanoic acid hydroxyamide (10b)

White powder, yield 46%, mp = 170–172 °C; ^{1}H NMR (600 MHz, DMSO-d_6): δ 10.68 (s, 1H), 8.80 (s, 1H), 7.42 (d, 1H, J = 7.2 Hz), 7.31 (m, 2H), 7.27 (m, 1H), 6.48 (t, 1H, J = 6.0 Hz), 6.27 (d, 1H, J = 9.0 Hz), 4.26 (d, 2H, J = 6.0 Hz), 4.08 (m, 1H), 1.54 (m, 1H), 1.34 (t, 2H, J = 7.2 Hz), 0.86 (dd, 6H, J = 6.6, 11.4 Hz); HRMS (AP-ESI) m/z Calcd for $C_{14}H_{20}ClN_3O_3$, $[M+H]^+$ 314.1266. Found, 314.1263.

5.2.10. (*S*)-2-[3-(2-Bromo-benzyl)-ureido]-4-methyl-pentanoic acid hydroxyamide (10c)

White powder, yield 56%, mp = 173–174 °C; ^{1}H NMR (600 MHz, DMSO-d_6): δ 10.68 (s, 1H), 8.80 (s, 1H), 7.28 (m, 2H), 7.17 (m, 2H), 6.42 (t, 1H, J = 6.0 Hz), 6.19 (d, 1H, J = 9.0 Hz), 4.24 (d, 2H, J = 6.0 Hz), 4.08 (m, 1H), 1.54 (m, 1H), 1.34 (t, 2H, J = 7.2 Hz), 0.89 (dd, 6H, J = 6.6, 10.8 Hz); HRMS (AP-ESI) m/z Calcd for $C_{14}H_{20}BrN_3O_3$, $[M+H]^+$ 358.0761. Found, 358.0763.

5.2.11. (*S*)-4-Methyl-2-[3-(2-methyl-benzyl)-ureido]-pentanoic acid hydroxyamide (10d)

White powder, yield 49%, mp = 162–164 °C; ^{1}H NMR (600 MHz, DMSO-d_6): δ 10.68 (s, 1H), 8.80 (s, 1H), 7.18 (m, 4H), 6.29 (t, 1H, J = 5.4 Hz), 6.09 (d, 1H, J = 9.0 Hz), 4.17 (d, 2H, J = 5.4 Hz), 4.09 (m, 1H), 2.25 (s, 1H), 1.54 (m, 1H), 1.34 (t, 2H, J = 7.2 Hz), 0.86 (dd, 6H, J = 6.6, 8.4 Hz); HRMS (AP-ESI) m/z Calcd for $C_{15}H_{23}N_3O_3$, $[M+H]^+$ 294.1812. Found, 294.1811.

5.3. General procedure for the synthesis of 9a–9g and 11a–11b

Corresponding *meta*-substituted anilines or benzylamines (15 mmol) was added to a solution of triphosgene (2.22 g, 7.5 mmol) in dry toluene (80 mL) in room temperature. The reaction mixture was refluxed for 4 h and then solvents removed under low pressure. The residue was dissolved in DCM (20 mL) and this solution was added to the mixture of L-leucine methyl ester hydrochloride (2.72 g, 15 mmol) and triethylamine (1.52 g, 15 mmol) in DCM (80 mL) under ice-bath. After stirred at room temperature for 12 min, the reaction mixture was concentrated under vacuum and then ethyl acetate (20 mL) was added to the residue. The organic phase was washed with 1 N HCl (10 mL) and saturated brine (10 mL) and dried with $MgSO_4$. After the solvent removed under low pressure, the residue without purification was directly added to a solution of potassium hydroxylamine (8.37 g, 56 mmol) in methanol (20 mL). The reaction mixture was stirred at room temperature for 1 h and then removed methanol under low pressure. The residue was taken up with 1 N HCl and extracted with ethyl acetate. The organic phase was washed with brine and dried with $MgSO_4$. After the solvent removed under low pressure, the residue was separated by silica gel column chromatography to afford **9a–9g** and **11a–11b**, respectively.

5.3.1. (*S*)-2-[3-(3-Fluoro-phenyl)-ureido]-4-methyl-pentanoic acid hydroxyamide (9a)

White powder, yield 43%, mp = 186–187 °C; ^{1}H NMR (600 MHz, DMSO-d_6): δ 10.81 (s, 1H), 8.88 (s, 1H), 8.78 (s, 1H), 7.43 (m, 1H), 7.24 (q, 1H, J = 7.8 Hz), 6.97 (d, 1H, J = 8.4 Hz), 6.71 (m, 1H), 6.411 (t, 1H, J = 8.4 Hz), 4.14 (m, 1H), 1.59 (m, 1H), 1.42 (t, 2H, J = 7.2 Hz), 0.89 (dd, 6H, J = 6.6, 10.8 Hz); HRMS (AP-ESI) m/z Calcd for $C_{13}H_{18}FN_3O_3$, $[M+H]^+$ 284.1405. Found, 284.1402.

5.3.2. (*S*)-2-[3-(3-Chloro-phenyl)-ureido]-4-methyl-pentanoic acid hydroxyamide (9b)

White powder, yield 47%, mp = 178–180 °C; ^{1}H NMR (600 MHz, DMSO-d_6): δ 10.76 (s, 1H), 8.85 (s, 1H), 8.72 (s, 1H), 7.61 (s, 1H), 7.20 (t, 1H, J = 7.8 Hz), 7.09 (d, 1H, J = 9.0 Hz), 6.90 (d, 1H, J = 7.8 Hz), 6.39 (d, 1H, J = 9.0 Hz), 4.09 (m, 1H), 1.54 (m, 1H), 1.37 (t, 2H, J = 7.2 Hz), 0.86 (dd, 6H, J = 5.4, 6.6 Hz); HRMS (AP-ESI) m/z Calcd for $C_{13}H_{18}ClN_3O_3$, $[M+H]^+$ 300.1109. Found, 300.1105.

5.3.3. (*S*)-2-[3-(3-Bromo-phenyl)-ureido]-4-methyl-pentanoic acid hydroxyamide (9c)

White powder, yield 60%, mp = 168–170 °C; ^{1}H NMR (600 MHz, DMSO-d_6): δ 10.81 (s, 1H), 8.85 (s, 1H), 8.74 (s, 1H), 7.79 (s, 1H), 7.17 (m, 2H), 7.07 (d, 1H, J = 6.6 Hz), 6.42 (d, 1H, J = 8.4 Hz), 4.16 (m, 1H), 1.57 (m, 1H), 1.42 (t, 2H, J = 7.2 Hz), 0.89 (dd, 6H, J = 5.4, 6.6 Hz); HRMS (AP-ESI) m/z Calcd for $C_{13}H_{18}BrN_3O_3$, $[M+H]^+$ 344.0604. Found, 344.0599.

5.3.4. (*S*)-4-Methyl-2-(3-*m*-tolyl-ureido)-pentanoic acid hydroxyamide (9d)

White powder, yield 61%, mp = 160–162 °C; ^{1}H NMR (600 MHz, DMSO-d_6): δ 10.70 (s, 1H), 8.78 (s, 1H), 8.41 (s, 1H), 7.14 (m, 3H), 6.71 (d, 1H, J = 7.8 Hz), 6.27 (d, 1H, J = 7.8 Hz), 4.14 (m, 1H), 2.25 (s, 3H), 1.59 (m, 1H), 1.42 (t, 2H, J = 7.2 Hz), 0.90 (dd, 6H, J = 6.6, 10.8 Hz); HRMS (AP-ESI) m/z Calcd for $C_{14}H_{21}N_3O_3$, $[M+H]^+$ 280.1656. Found, 280.1653.

5.3.5. (*S*)-2-[3-(3-Methoxy-phenyl)-ureido]-4-methyl-pentanoic acid hydroxyamide (9e)

White powder, yield 55%, mp = 172–174 °C; ^{1}H NMR (600 MHz, DMSO-d_6): δ 10.79 (s, 1H), 8.89 (s, 1H), 8.55 (s, 1H), 7.13 (m, 2H), 6.81 (d, 1H, J = 7.8 Hz), 6.48 (dd, 1H, J = 1.8, 6 Hz), 6.32 (d, 1H, J = 9.0 Hz), 4.12 (m, 1H), 3.69 (s, 1H), 1.57 (m, 1H), 1.39 (t, 2H, J = 7.2 Hz), 0.89 (dd, 6H, J = 6.6, 10.8 Hz); HRMS (AP-ESI) m/z Calcd for $C_{14}H_{21}N_3O_4$, $[M+H]^+$ 296.1605. Found, 296.1599.

5.3.6. (*S*)-4-Methyl-2-[3-(3-trifluoromethyl-phenyl)-ureido]-pentanoic acid hydroxyamide (9f)

White powder, yield 40%, mp = 173–174 °C; ^{1}H NMR (600 MHz, DMSO-d_6): δ 10.73 (s, 1H), 8.88 (s, 1H), 8.80 (s, 1H), 7.95 (s, 1H), 7.45 (m, 2H), 7.23 (d, 1H, J = 7.8 Hz), 6.41 (d, 1H, J = 7.8 Hz), 4.16 (m, 1H), 1.44 (m, 1H), 1.39 (t, 2H, J = 7.2 Hz), 0.91 (dd, 6H, J = 6.6, 10.8 Hz); HRMS (AP-ESI) m/z Calcd for $C_{14}H_{18}F_3N_3O_3$, $[M+H]^+$ 334.1373. Found, 334.1372.

5.3.7. (*S*)-2-[3-(3-Hydroxy-phenyl)-ureido]-4-methyl-pentanoic acid hydroxyamide (9g)

White powder, yield 41%, mp = 122–124 °C; ^{1}H NMR (600 MHz, DMSO-d_6): δ 10.79 (s, 1H), 9.21 (s, 1H), 8.84 (s, 1H), 8.41 (s, 1H), 6.98 (m, 2H), 6.70 (d, 1H, J = 7.8 Hz), 6.27 (m, 2H), 6.32 (d, 1H, J = 9.0 Hz), 4.12 (m, 1H), 1.57 (m, 1H), 1.39 (t, 2H, J = 7.2 Hz), 0.89 (dd, 6H, J = 6.6, 10.8 Hz); HRMS (AP-ESI) m/z Calcd for $C_{14}H_{19}N_3O_4$, $[M+H]^+$ 282.1448. Found, 282.1448.

5.3.8. (*S*)-2-[3-(3-Chloro-benzyl)-ureido]-4-methyl-pentanoic acid hydroxyamide (11a)

White powder, yield 49%, mp = 166–167 °C; ^{1}H NMR (600 MHz, DMSO-d_6): δ 10.68 (s, 1H), 8.80 (s, 1H), 7.33 (t, 1H, J = 7.8 Hz), 7.27 (m, 2H), 7.18 (d, 1H, J = 7.8 Hz), 6.48 (t, 1H, J = 6.0 Hz), 6.19 (d, 1H, J = 8.4 Hz), 4.22 (d, 2H, J = 6.0 Hz), 4.09 (m, 1H), 1.54 (m, 1H), 1.35 (t, 2H, J = 7.2 Hz), 0.86 (dd, 6H, J = 6.6, 8.4 Hz); HRMS (AP-ESI) m/z Calcd for $C_{14}H_{20}ClN_3O_3$, $[M+H]^+$ 314.1266. Found, 314.1269.

5.3.9. (*S*)-4-Methyl-2-[3-(3-methyl-benzyl)-ureido]-pentanoic acid hydroxyamide (11b)

White powder, yield 53%, mp = 162–163 °C; ^{1}H NMR (600 MHz, DMSO-d_6): δ 10.68 (s, 1H), 8.80 (s, 1H), 7.19 (t, 1H, J = 7.8 Hz), 7.02 (m, 3H), 6.37 (t, 1H, J = 6.0 Hz), 6.11 (d, 1H, J = 9.0 Hz), 4.16 (d, 2H, J = 6.0 Hz), 4.09 (m, 1H), 2.28 (s, 3H), 1.55 (m, 1H), 1.35 (t, 2H, J = 7.2 Hz), 0.86 (dd, 6H, J = 6.6, 8.4 Hz); HRMS (AP-ESI) m/z Calcd for $C_{15}H_{23}N_3O_3$, $[M+H]^+$ 294.1812. Found, 294.1815.

5.4. Biological evaluation

5.4.1. In vitro APN inhibition assay

IC_{50} values against APN were determined by using L-leu-*p*-nitroanilide as substrate and Microsomal aminopeptidase from Porcine Kidney Microsomes (Sigma) as enzyme in 50 mM PBS (PH 7.2) or suspension of **ES-2** cells in PBS (1×10^5/well). After adding the detected compounds, the solution with various concentrations was incubated with APN at 37 °C for 5 min. Then the solution of substrate was added into the above mixture, which was incubated for another 30 min at 37 °C. The hydrolysis of the substrate was measured by following the change in the absorbance monitored at 405 nm with a plate reader (Varioskan, Thermo, USA).

5.4.2. In vitro HDACs inhibition assay

In vitro HDACs inhibitory activity assay was determined by using Boc-Lys (acetyl)-AMC as substrate and Hela nuclear extract (containing HDAC1, HDAC3, HDAC5 and HDAC8) as enzymes in 15 mM Tris–HCl (PH 8.0) at 37 °C. First, 10 μL of enzymes solution was added to tested compounds solutions at various concentrations (50 μL) and incubated for 5 min at 37 °C. Then 40 μL of substrate was added and the mixture continued to incubate for another 30 min in the same environment. Finally, 100 μL of developer which containing trypsin and TSA was putted into the mixture. Twenty minutes later, fluorescence intensity was measured at 390 nm excitation and 460 nm emission wavelengths with a microplate reader.

5.4.3. MTT assay

ES-2 cell and **U-937** cell were grown in RPMI1640 medium with 10 FBS at 37 °C in 5% CO_2 humidified incubator. Cell proliferation was determined by MTT [(3-[4,5-dimethyl-2-thiazolyl]-2,5-diphenyl-2*H*-tetrazolium bromide)] method. In brief, cells were pated in 96-well plates (5000/well) and cultivated for 4 h, and then different concentrations of inhibitors were added. Followed by another 48 h treatment, 1% MTT was added each well. Four hours later, DMSO was added and mixed for 15 min. Finally, the optical density values were monitored at 570 nm.

Acknowledgments

This work was supported by National Science and Technology Specific Projects of China (No. 2011ZX09401-015) and National Nature Science Foundation of China (No. 21172134).

References and notes

1. Fukasawa, K.; Fujii, H.; Saitoh, Y.; Koizumi, K.; Aozuka, Y.; Sekine, K.; Yamada, M.; Saiki, I.; Nishikawa, K. *Cancer Lett.* **2006**, *243*, 135.
2. Luan, Y.; Xu, W. *Curr. Med. Chem.* **2007**, *14*, 639.
3. Saiki, I.; Yoneda, J.; Azuma, I.; Fujii, H.; Abe, F.; Nakajima, M.; Tsuruo, T. *Int. J. Cancer* **1993**, *54*, 137.
4. Rangel, R.; Sun, Y.; Guzman-Rojas, L.; Ozawa, M. G.; Sun, J.; Giordano, R. J.; Van Pelt, C. S.; Tinkey, P. T.; Behringer, R. R.; Sidman, R. L.; Arap, W.; Pasqualini, R. *Proc. Natl. Acad. Sci. U.S.A.* **2007**, *104*, 4588.
5. Umezawa, H.; Aoyagi, T.; Suda, H.; Hamada, M.; Takeuchi, T. *J. Antibiot.* **1976**, *29*, 97.
6. Aoyagi, T.; Yoshida, S.; Nakamura, Y.; Shigihara, Y.; Hamada, M.; Takeuchi, T. *J. Antibiot.* **1990**, *43*, 143.
7. Rich, D. H.; Moon, B. J.; Harbeson, S. *J. Med. Chem.* **1984**, *27*, 417.
8. Umezawa, H. A.; Aoyagi, T.; Tanaka, T.; Suda, H. *J. Antibiot.* **1985**, *38*, 1629.
9. Nagai, M. K. F.; Naganawa, H. *J. Antibiot.* **1997**, *50*, 82.
10. Lampret, B. R. K. J.; Kralj, B. *Arch. Microbiol.* **1999**, *171*, 397.
11. Chung, M. C.; Lee, H. J.; Chun, H. K.; Lee, C. H.; Kim, S. I.; Kho, Y. H. *Biosci., Biotechnol., Biochem.* **1996**, *60*, 898.
12. Aoyagi, T.; Yoshida, S.; Matsuda, N.; Ikeda, T.; Hamada, M.; Takeuchi, T. *J. Antibiot.* **1991**, *44*, 573.
13. Wang, Q.; Chen, M.; Zhu, H.; Zhang, J.; Fang, H.; Wang, B.; Xu, W. *Bioorg. Med. Chem.* **2008**, *16*, 5473.
14. Tu, G.; Li, S.; Huang, H.; Li, G.; Xiong, F.; Mai, X.; Zhu, H.; Kuang, B.; Xu, W. F. *Bioorg. Med. Chem.* **2008**, *16*, 6663.
15. Li, X.; Wang, J.; Li, J.; Wu, J.; Li, Y.; Zhu, H.; Fan, R.; Xu, W. *Bioorg. Med. Chem.* **2009**, *17*, 3053.
16. Yang, K.; Wang, Q.; Su, L.; Fang, H.; Wang, X.; Gong, J.; Wang, B.; Xu, W. *Bioorg. Med. Chem.* **2009**, *17*, 3810.
17. Mou, J.; Fang, H.; Jing, F.; Wang, Q.; Liu, Y.; Zhu, H.; Shang, L.; Wang, X.; Xu, W. *Bioorg. Med. Chem.* **2009**, *17*, 4666.
18. Jin, K.; Zhang, X.; Ma, C.; Xu, Y.; Yuan, Y.; Xu, W. *Bioorg. Med. Chem.*<http://dx.doi.org/10.1016/j.bmc.2012.06.024>
19. Su, L.; Jia, Y.; Zhang, L.; Xu, Y.; Fang, H.; Xu, W. *Bioorg. Med. Chem.* **2012**, *20*, 3807.
20. Su, L.; Cao, J.; Jia, Y.; Zhang, X.; Fang, H.; Xu, W. *ACS Med. Chem. Lett.* **2012**, *3*, 959.